

EXPERIMENTAL

Material preparation

Preparation of the Oxygen Cathode

The carbon cloth was first treated in the concentrated nitric acid (69%) at 120 °C for 12 hours. Equivoluminal $\text{Co}(\text{NO}_3)_2$ (50 mM) and 2-Methylimidazole (0.4 M) aqueous solutions were mixed to form 80 mL under continuous stirring. Then the carbon cloth was immersed into the above solution and aged for 2 hours. After that, the sample was rinsed with deionized water and ethyl alcohol, followed by drying at 60 °C overnight. The $\text{Ni}(\text{NO}_3)_2$ (0.2 g) was dissolved in 100 mL ethyl alcohol. The dried sample was immersed in the above solution for etching. The Ni ion will hydrolyze and generate the H^+ , which can etch the MOF. As a result, the NiCo-LDH is formed on the carbon textile. By adjusting immersing time, the loading of nickel element was accurately controlled without structural destroy. The final products are obtained by calcining in air at 350 °C for 2 hours with heating rate of 1 °C min^{-1} . The samples were named as NCO-CT and the mass loading of the NCO is about 0.13 mg cm^{-2} . In comparison, the CO-CT sample was obtained without nickel ion etching.

Synthesis of Solid-state Electrolyte

The stoichiometric amount of Li_2CO_3 , Al_2O_3 , GeO_2 and $\text{NH}_4\text{H}_2\text{PO}_4$ was first grinded to initially mix. Then the powder was transferred for high-energy ball miller (Pulverisette-7) as at 400 rpm. The mass ratio of the ZrO_2 balls (diameter: 5mm) to precursors is 4:1. After milling for 4 hours, the mixed powder was calcined in air to release gas (NH_3 and CO_2) at 600 °C for 1 hour with heating rate of 1 °C min^{-1} . Afterwards, continuing high-energy ball milling at 400 rpm was conducted for another 4 hours. The LAGP was obtained by sintering at 900 °C for 6 hours. To obtain the LAGP pellet, the ceramic bulks were milled into powders and extruded into nummular pellet. The final products were treated at 900 °C for 6 hours and the size were pressed into pellet with a diameter of 10 mm and thickness of 1 mm.

Structural and morphological characterization

Thermogravimetric (TG)/Differential Thermal Analysis (DTA) on a PerkinElmer TGA 7 instrument was used to obtain the loading content of the active material on the carbon textile in air from room temperature to 1000 °C. Powder X-ray diffraction data was collected using Rigaku RINT-2200 diffractometer. The morphological information of the NCO-CT samples was analyzed by Scanning Electron Microscopy (SEM, JEM-2100F), Field-emission Scanning Electron Microscopy (FE-SEM, FEI Quanta 400), and High-resolution Transmission Electron Microscopy (HR-TEM, Hitachi H-800). The chemical compositions of the surfaces of the NCO-CT were examined by X-ray photoelectron spectroscopy (XPS, Thermo VG scientific).

Electrochemical Measurements

The NCO-CT and CO-CT samples are directly used as the oxygen electrode by cutting into disc of 8 mm. The LAGP solid-state electrolyte serves as the separator and metal lithium works as anode. Then the samples were assembled into Swagelok cell. Noted that here we added 20 μL organic electrolyte (1 M Bis(trifluoromethane)sulfonimide lithium salt in tetraethylene glycol dimethyl ether) to guarantee the Li^+ transfer in oxygen electrode. All the samples were vacuum drying overnight and assembling processes were performed in an Ar-filled glove box (water and oxygen lower than 1 ppm). The assembled solid-state LOBs were pumped with 0.1 MPa pure oxygen (99.999%).

The Galvanostatic discharge/charge performance were carried out on a standard battery test instrument (Hokuto Denko Corporation, HJ1001SD8) and all current density is based on mass loading of NiCo_2O_4 . The ionic conductivity of the LAGP nummular pellets were characterized by blocking of mobile Li ions with Pt. And then electrochemical AC impedance spectroscopy (EIS) of the LAGP nummular pellets was obtained by electrochemical workstation (Solartron 1287 coupled with Solartron 1260) under open-circuit voltage in the frequency range of 10^5 Hz to 10^{-2} Hz with an AC amplitude of 10 mV.

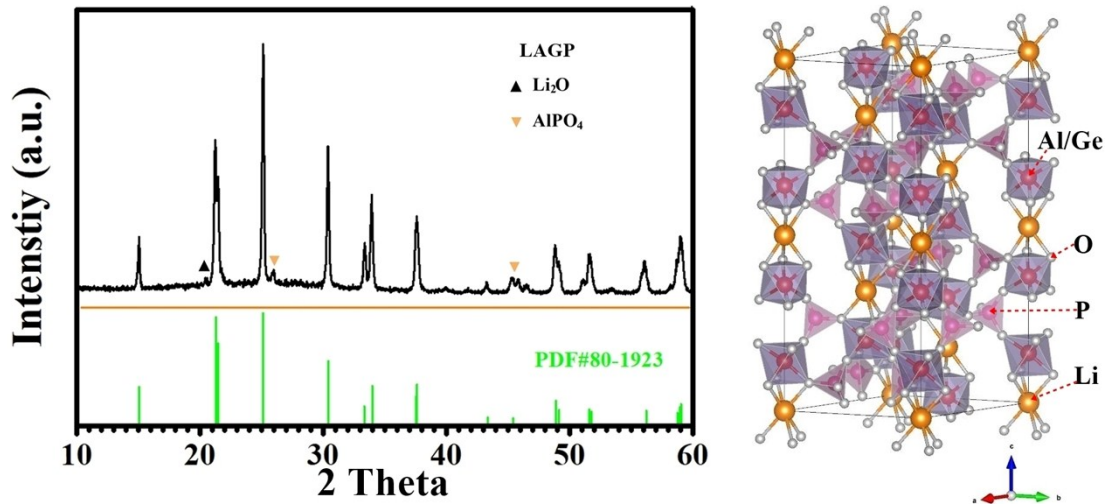


Fig. S1. The XRD pattern of the solid-state LAGP electrolytes and standard PDF card for $\text{LiGe}_2(\text{PO}_4)_3$ (no. 80-1923)

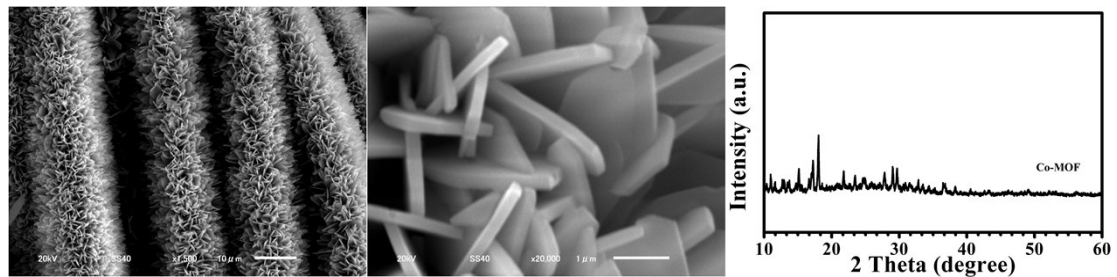


Fig. S2. The SEM image and XRD curve of the Co-MOF before treated with $\text{Ni}(\text{NO}_3)_2$ in ethyl alcohol.

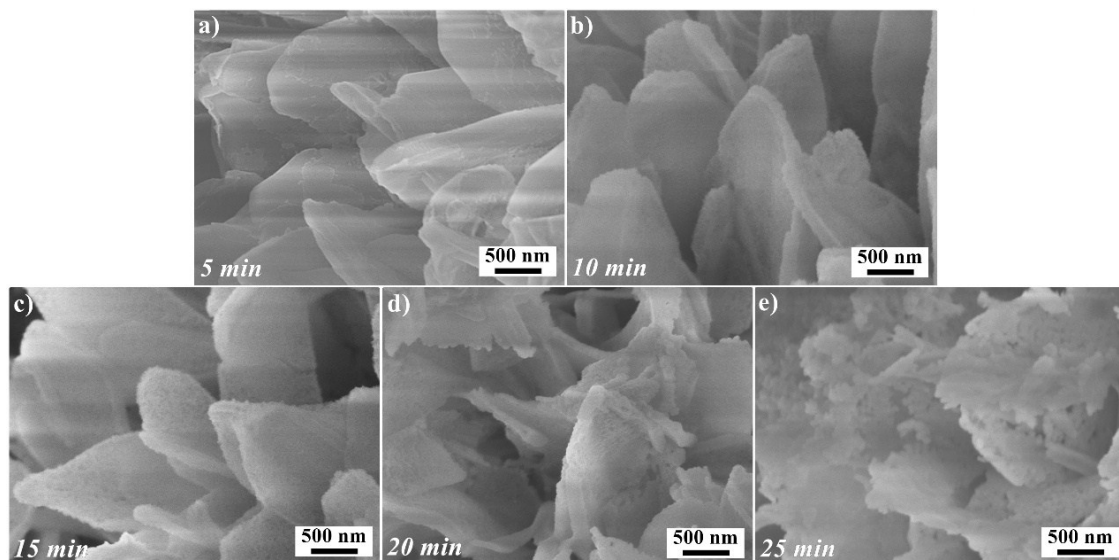


Fig. S3. The CO-MOF immersed in $\text{Ni}(\text{NO}_3)_2$ of ethyl alcohol solution for different time: 5 min (a); 10 min (b); 15 min (c); 20 min (d); 25 min (e).

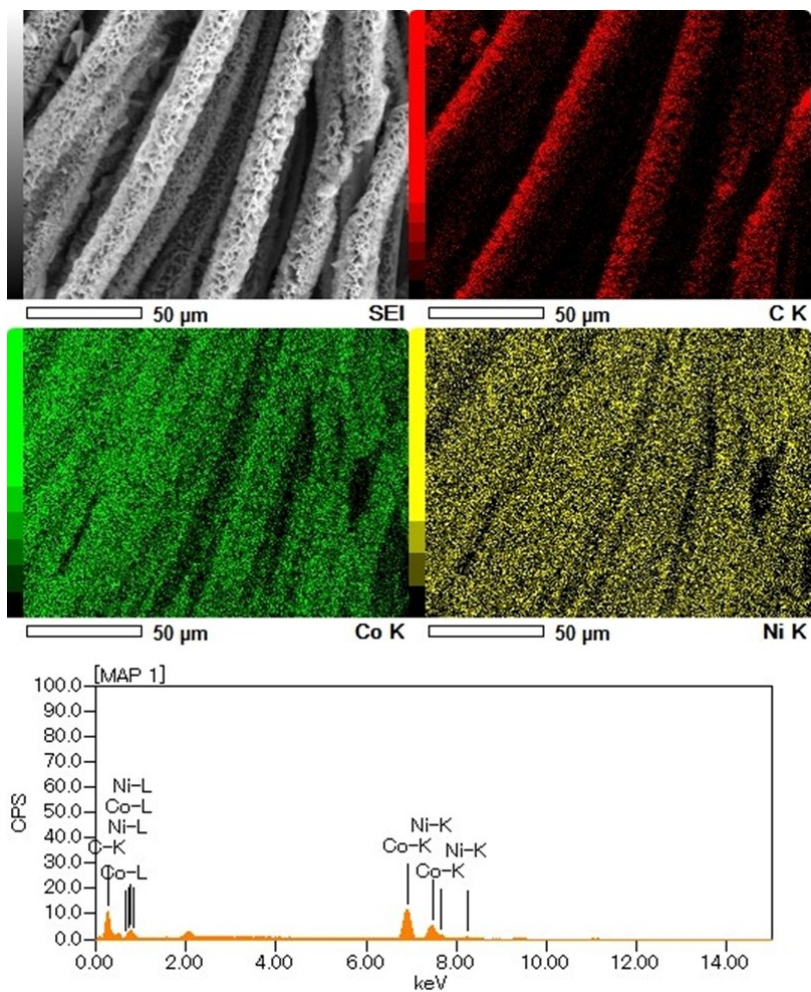


Fig. S4. Mapping result of the Ni-treated Co-MOF and the corresponding EDX curve, obtained in the SEM analysis.

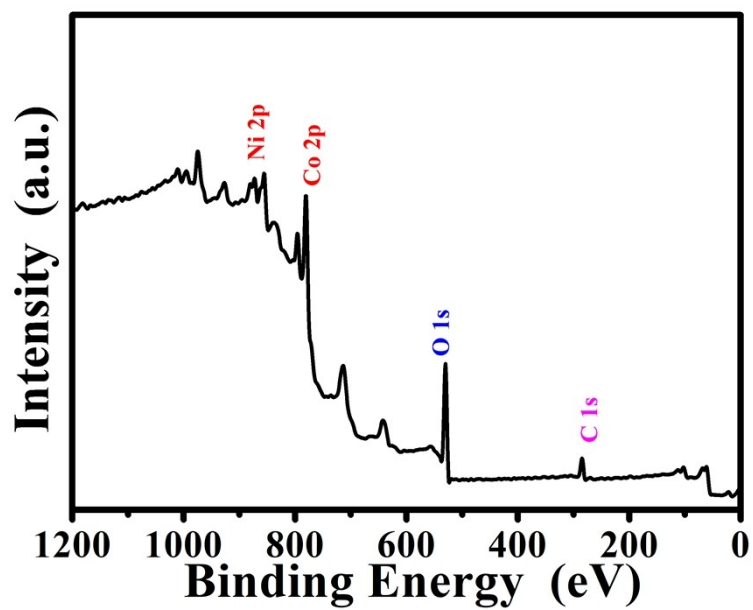


Fig. S5. X-ray photoelectron spectroscopy (XPS) survey spectrum of NCO-CT samples.

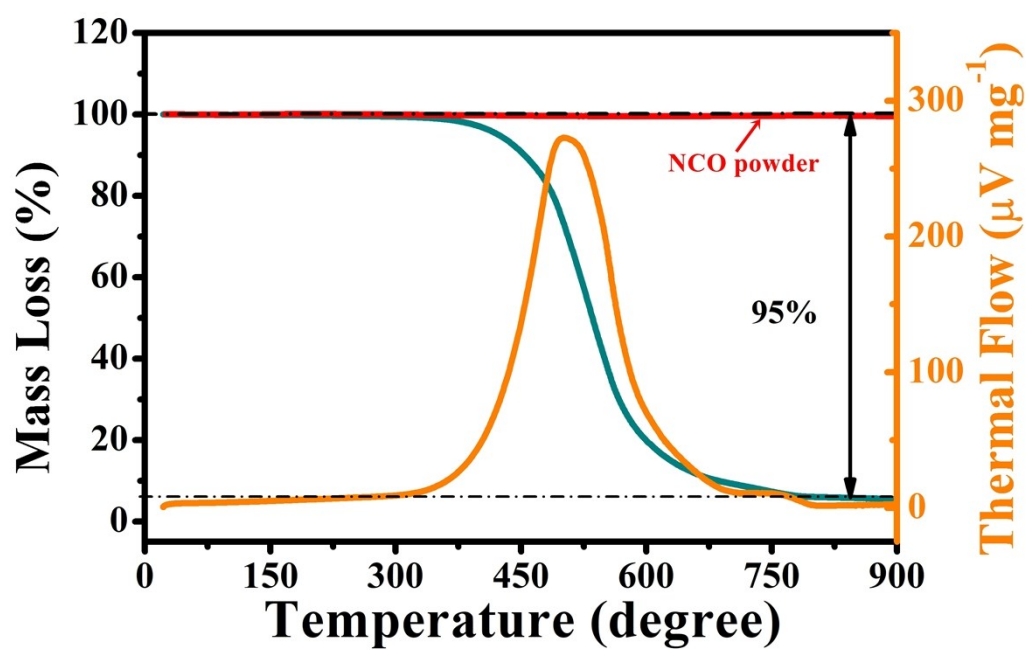


Fig. S6. The TG and DSC curves of NCO-CT cathode calcined in a temperature range from room temperature to 900 °C under O_2 atmosphere.

Table S1. Electrochemical performance of the NCO-CT cathode in this study, compared with some other reported oxygen cathode in previous literatures.

Reference	Type of electrolyte	Cathode	Current density	Limited capacity	Cycle number
This work	$\text{Li}_{1+x}\text{Al}_x\text{Ge}_{2-x}(\text{PO}_4)_3$	MOF-converted NiCo_2O_4	100 mA g^{-1}	500 mAh g^{-1}	90
1	PVDF-HFP polymer matrix	carbon black	50 mA g^{-1}	500 mAh g^{-1}	50
2	LATP	carbon black	100 mA g^{-1}	500 mAh g^{-1}	14
3	Liquid Electrolyte	TiCrOx	50 mA g^{-1}	200 mAh g^{-1}	20
4	Liquid Electrolyte	$\text{NiCo}_2\text{O}_4 @ \text{Co}_3\text{O}_4$	100 mA g^{-1}	500 mAh g^{-1}	60
5	PEO	Carbon	-	500 mAh g^{-1}	20
6	PVDF-HFP	Carbon	0.25 mA cm^{-2}	10 mAh	30
7	Liquid Electrolyte	Co/CoO-Graphene	100	500 mAh g^{-1}	70
8	LiTFSI/TEGDME	MOF-converted carbon	20 mA g^{-1}	500 mAh g^{-1}	74
9	LiTFSI/TEGDME	NiCo_2O_4	200 mA g^{-1}	1000 mAh g^{-1}	30
10	LiTFSI/TEGDME	ZnCo_2O_4 nanoflakes	0.1 mA cm^{-2}	500 mAh g^{-1}	30
11	LiTFSI/TEGDME	NiCo_2O_4	0.02 mA cm^{-2}	500 mAh g^{-1}	16
12	LIFSI/ TEGDEM	NiCo_2O_4	0.1 mA cm^{-2}	1000 mAh g^{-1}	20

References:

1. J. Zhang, B. Sun, X. Xie, K. Kretschmer and G. Wang, *Electrochim. Acta*, **2015**, 183, 56-62.
2. X. Wang, D. Zhu, M. Song, S. Cai, L. Zhang and Y. Chen, *ACS Appl. Mater. Inter.*, **2014**, 6, 11204-11210.
3. N-C. Lai, G. Cong, Z. Liang and Y-C. Lu, *Joule*, **2018**, 2, 1511-1521.
4. P. Sennu, H. S. Park, K. U. Park, V. Aravindan, K. S. Nahm and Y.-S. Lee. *J. Catalysis*, **2017**, 349, 175-182.
5. G. A. Elia and J. Hassoun, *Sci. Rep.*, **2015**, 5, 12307

6. K.-N. Jung, J.-I. Lee, J.-H. Jung, K.-H. Shin and J.-W. Lee, *Chem. Commun.*, **2014**, 50, 5458-5461.
7. P. Zhang, R. Wang, M. He, J. Lang, S. Xu and X. Yan, *Adv. Funct. Mater.*, **2016**, 26, 1354-1364.
8. H. T. T. Pham, Y. Kim, Y-J Kim, J-W Lee and M-S Park, *Adv. Funct. Mater.*, **2019**, 1902915.
9. B. Sun, X. D. Huang, S. Q. Chen, Y. F. Zhao, J. Q. Zhang, P. Munroe and G. X. Wang, *J. Mater. Chem. A* **2014**, 2, 12053-12059.
10. T. F. Hung, S. G. Mohamed, C. C. Shen, Y. Q. Tsai, W. S. Chang and R. S. Liu, *Nanoscale*, **2013**, 5, 12115–12119.
11. J. Yuan, Z. Liu, Y. Wen, H. Hu, Y. Zhu and V. Thangadurai, *Ionics*, **2019**, 25, 1669-1677.
12. Y. Li, L. Zou, J. Li, K. Guo, X. Dong, X. Li, X. Xue, H. Zhang and H. Yang, *Electrochim. Acta*, **2019**, 129, 14-20